Desalination and Water Treatment
www.deswater.com
doi: 10.5004/dwt.2021.26837

219 (2021) 187–195
April

Power supply stability of marine aquaculture based on DC brushless generator

Wenjuan Zhang, Zhigang Zhang*

College of Electronic Communication and Electrical Engineering, Changsha University, Changsha 410022, China, email: zwjs0909@sina.com (Z. Zhang)

Received 15 August 2020; Accepted 23 November 2020

ABSTRACT

In order to improve the power supply stability of the marine aquaculture DC brushless generator, a power supply stability control method of the marine aquaculture DC brushless generator based on multi-parameter fusion decoupling regulation is proposed, a control constraint parameter model of the marine aquaculture DC brushless generator is constructed, and an output load oscillation regulation method is adopted to carry out DC brushless adaptive steady-state regulation of the marine aquaculture DC brushless generator. A DC brushless adaptive coupling model of marine aquaculture DC brushless generators between different frequency systems is established. Multidimensional parameter adaptive fusion and steady-state tracking methods are used to adjust DC brushless adaptive gain, and DC harmonic dynamic suppression of marine aquaculture DC brushless generators is carried out to realize power supply stability control. The simulation results show that the output stability and output power gain of the DC brushless generator used in marine aquaculture are better and the optimal distribution control capability of marine aquaculture power supply is improved.

Keywords: DC brushless generator; Marine aquaculture; Power supply; Stability

1. Introduction

Marine aquaculture DC brushless generators are widely used in high-power power generation and transmission systems, and marine aquaculture DC brushless generators represented by photovoltaic power generation are widely used in DC transformers [1]. By the multi-power decentralized control design of marine aquaculture DC brushless generators, the output power gain and stability of marine aquaculture DC brushless generators are improved, and the power supply stability control method of marine aquaculture DC brushless generators is studied, which is of great significance in improving the energy access collection capability and high-voltage and high-power regulation capability of power supply systems [2].

The research on the power supply stability of marine aquaculture DC brushless generator is based on the DC brushless adaptive modulation and power factor analysis, combined with the inverter rapid response design of marine aquaculture DC brushless generator, to carry out two-way rapid continuous regulation of power generation power, and to improve the power supply stability of marine aquaculture DC brushless generator. In the traditional method, the power supply stability control methods of marine aquaculture DC brushless generator mainly include adaptive fuzzy control method, steady-state power modulation method, and maximum equalization interval control method [3]. In view of the above problems, this paper proposes a power supply stability control method for marine aquaculture DC brushless generator based on multi-parameter fusion decoupling regulation, constructs a control constraint parameter model for marine aquaculture DC brushless generator, adopts output load oscillation regulation method for DC brushless generator DC

* Corresponding author.

brushless adaptive steady-state regulation, establishes a DC brushless adaptive coupling model of marine aquaculture DC brushless generator between different frequency systems, uses multi-dimensional parameter adaptive fusion, and steady-state tracking method for DC brushless adaptive gain regulation of marine aquaculture DC generator, and realizes power supply stability control. Finally, the simulation results show the superior performance of this method in improving the power supply stability of marine aquaculture DC brushless generator [4].

2. Control object and constraint parameters of marine aquaculture DC brushless generator

2.1. Analysis of rectifier output voltage waveform

The brushless DC generator is composed of four pairs of pole 48 slot tangential structure permanent magnet synchronous generator and a new 12-phase zero-type rectifier circuit. The stator of the tangential structure permanent magnet synchronous motor is mainly composed of stator core and armature winding, and the rotor is mainly composed of non-magnetic guard ring, permanent magnet magnetic steel, NS pole boot, non-magnetic guide bushing, and rotary shaft, as shown in Fig. 1. The permanent magnet embedded in the rotor is tangentially magnetized, and

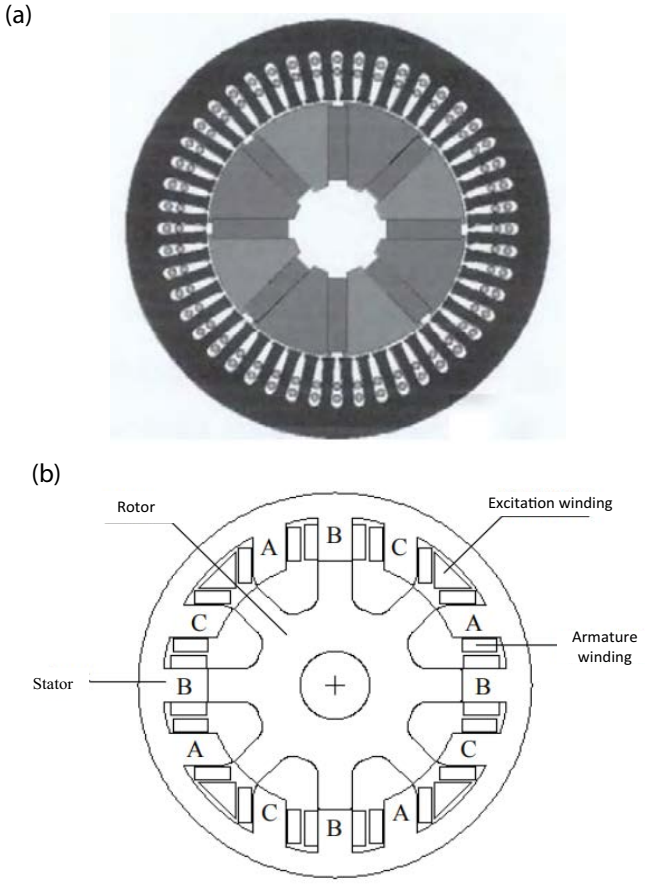

Fig. 1. DC brushless generator section: (a) physical sectional drawing and (b) inner structure.

there are two corresponding permanent magnet truncated face air gap to provide per pole flux, so the air gap magnetic induction intensity of the motor can be effectively improved.

The rectifier circuit of the electric excitation dual-salient generator system is shown in Fig. 2.

In Fig. 2, the diode D_1~D_6 constitutes a three-phase full-bridge uncontrolled rectifier; C_f is the filter capacitance; R is the discharge resistance; and R_L is the resistive load. The rectifier bridge front stage input is the generator three-phase AC output voltage, while the induced potential change frequency is proportional to the rotational speed n and the number of rotor teeth p, which can be expressed as $f_r = np/60$. The motor used in the experiment is a 12/8 structure with a rotational speed of 5,000 rpm, so the induction potential period is 1.5 ms. the simulation waveform in the light load state is shown in Fig. 3 (without filter capacitance). the output voltage through the rectifier bridge contains abundant harmonic components in addition to the DC component, where the lowest fundamental frequency is $f_1 = 3f_r$, implying the generation of 3 output voltage wave heads over a period of inductive potential change.

As can be seen from Fig. 3, if the phase-changing overlap is ignored in normal operation, the power-on sequence of the three-phase armature winding in an inductive potential cycle is as follows: $A + C- \rightarrow B + A- \rightarrow C + B-$, the conduction order of the corresponding rectifier diode is: D_1, $D_6 \rightarrow D_3$, $D_2 \rightarrow D_5$, D_4, each diode on 1/3 cycle. The following takes the resistive load case as an example to discuss the fault situation. The rectifier circuit fault is defined as a diode open circuit. This paper does not involve the diode short circuit fault, mainly for two reasons, one is that the overcurrent protection circuit will stop the rectifier circuit when the fault occurs, the other is that the diode fault is the most common open circuit.

2.2. Classification of operation status of rectifier circuits

When a fault occurs, the rectifier output voltage U_d produces distortion according to certain rules. For example, when D_1 fails, the diode conduction sequence becomes: D_3, $D_6 \rightarrow D_3$, $D_2 \rightarrow D_5$, D_4, U_d waveform is distorted in the first 1/3 cycle. When D_2 fails, the diode conduction sequence becomes: D_1, $D_6 \rightarrow D_3$, $D_6 \rightarrow D_5$, D_4, U_d waveform is distorted in the middle 1/3 cycle, so the D_2 fault rectifier voltage waveform is 120° behind the phase of the D_1 fault rectifier voltage waveform, but the waveform shape is similar. The D_3 fault rectifier voltage waveform is 120° behind the phase of the D_2 fault rectifier voltage waveform, and so on. When D_1, D_2 fails, the diode conduction sequence becomes: D_3, $D_6 \rightarrow D_3$, $D_6 \rightarrow D_5$, D_4, U_d waveform is distorted in the first 2/3 cycle, and its phase lag 1/3 cycle is obtained D_3, D_4 fault rectifier voltage waveform. The other kinds of fault element waveforms can be obtained by the same analysis method. According to the above U_d waveform distortion law, the operation state of the rectifier circuit of the electric excitation dual-salient generator system can be classified according to the following ways. Since there are two diodes with the highest probability of failure at the same time, based on this statistical rule, the fault is divided into seven types of 22 types of fault elements. Fig. 4 is the U_d waveform at the fault of class 2–7.

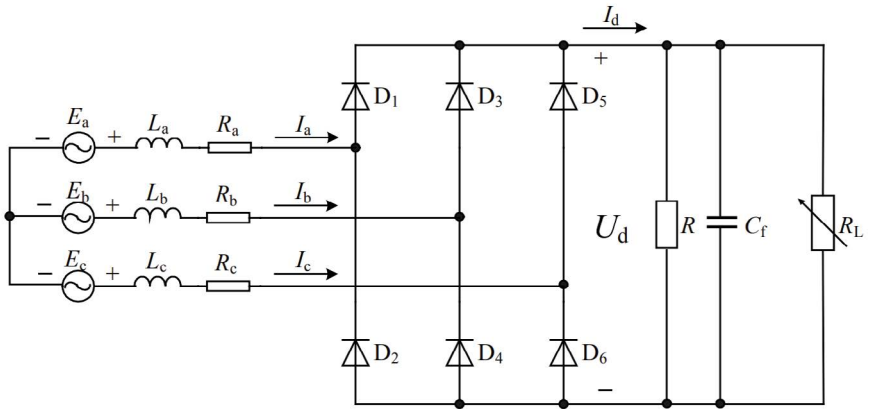

Fig. 2. Generator rectifier circuit.

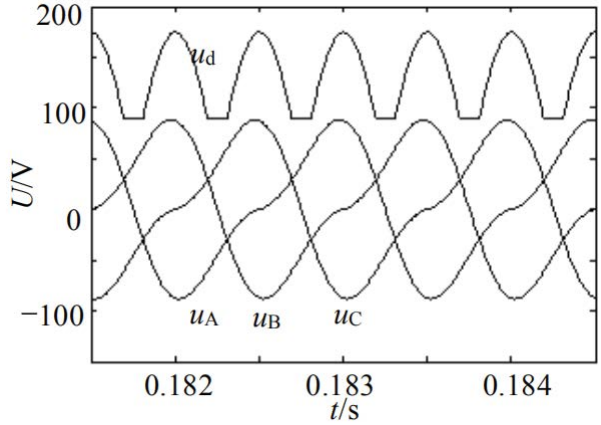

Fig. 3. Motor voltage and rectifier output waveform.

For the sake of intuition, only part of the sampling period is shown in the Fig. 4, and the waveform of different fault elements of the same fault class is similar, but there is a certain phase difference.

2.3. Controlled constraint parameters model of marine aquaculture DC brushless generator

In order to realize the power supply stability of DC brushless generator in marine aquaculture, the object model of power supply stability of DC brushless generator in marine aquaculture is constructed by PID controller. According to the unipolar characteristics of DC brushless generator in marine aquaculture [3], the differential control model of DC brushless generator in marine aquaculture is constructed with the following binary differential equations:

$$v(u) = L_Q\left(f(u) + \frac{1}{U_J}\int_0^u f(u)du + U_E\frac{df(u)}{du} \right) \tag{1}$$

In the Eq. (1), L_q denotes the controllable voltage source, U_J denotes the voltage with DC bias, and U_E is the high voltage side voltage. The marine aquaculture DC brushless generator control constraint characteristic quantity is expressed by Eq. (2):

$$\Delta v(l) = L_Q\Delta f(l) + L_J f(l) + L_E\left[\Delta f(l) - \Delta f(l-1)\right] \tag{2}$$

where L_q represents the generation interharmonic current of marine aquaculture DC brushless generator system, $L_J = \frac{L_q U}{U_J}$ is the frequency of load fluctuation, and $L_E = \frac{L_q U_E}{U}$ is the differential parameter of marine aquaculture DC brushless generator. Ignore the loss of the converter, use the fuzzy two-degree-of-freedom control model for the stability of the power supply of the marine aquaculture DC brushless generator, output the average power change rate G, calculate the DC control variable of the marine aquaculture DC brushless generator [5], adopt the upper and lower bridge-arm complementary mode, get the constrained object model of the power transmission:

$$\begin{bmatrix} G_{11}s(s) & G_{12}(s) \\ G_{21}(s) & G_{22}(s) \end{bmatrix} = \begin{bmatrix} \frac{1.7e^{-30s}}{7s+1} & \frac{0.59e^{-27s}}{8s+1} \\ \frac{-0.6e^{-25s}}{10s+1} & \frac{1.5e^{-28s}}{9s+1} \end{bmatrix} \tag{3}$$

A coupler between different frequency systems is constructed to meet the actual needs, and the stochastic volatility control equation is obtained:

$$\begin{cases} fh = fhan\left(x_1(k) - v(k), x_2(k), r, h_0\right) \\ x_1(k+1) = x_1(k) + hx_2(k) \\ x_2(k+1) = x_2(k) + hfh \end{cases} \tag{4}$$

In the Eq. (4), v is the DC voltage input signal; d_g is the input signal at the determined disturbance step; $\dot{x}$ is the first derivative of the input signal; df is the step of the double closed-loop control, using the joint control method of the outer loop and the current inner loop, the controlled DC instruction output filter factor is x_1, when the h value

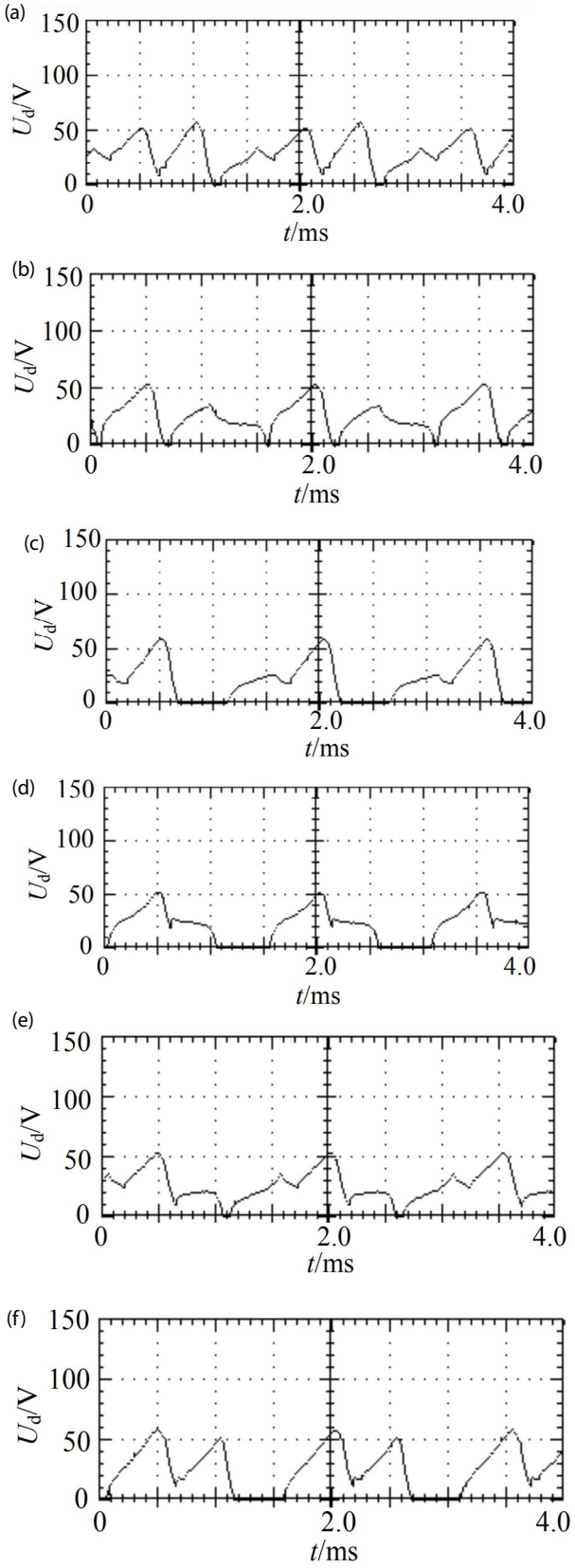

Fig. 4. Different types of fault rectifier voltage waveforms: (a) D_1 hitch, (b) D_1, D_2 hitch, (c) D_1, D_3 hitch, (d) D_2, D_4 hitch, (e) D_1, D_4 hitch, and (f) D_2, D_3 hitch.

is constant and the input voltage is stable, the X can be increased when the h_0 can be filtered; h_0 is the battery characteristic parameter of the marine aquaculture DC-culture brushless generator, and the DC-free brushless adaptive steady-state regulation of the marine aquaculture brushless DC generator is carried out by the method of load oscillation regulation [6].

2.4. Adaptive homeostasis regulation of DC brushless generator for marine aquaculture

Based on the above control constraint parameter model of marine aquaculture DC brushless generator, the state view model of DC brushless generator with output voltage and current command value is presented as:

$$\begin{cases} e = z_1 - y \\ \dot{z}_1 = z_2 - \beta_1 e \\ \dot{z}_2 = z_3 - \beta_2 \mathrm{fal}\left(e, 0.5, \delta\right) \\ \dot{z}_3 = -\beta_3 \mathrm{fal}\left(1, 0.25, \delta\right) + \mathbf{b}u \end{cases} \tag{5}$$

In the Eq. (5), z_1, z_2 is the maximum power point factor of DC brushless power generation in marine aquaculture, y is the characteristic parameter of DC brushless power generation in marine aquaculture, z_3 is the interference factor of maximum powerpoint to the system, and β_1, β_2, β_3, δ, and b is the adjustable parameter of DC brushless power generation in marine aquaculture [7].

Under the mode of inter-harmonic current frequency, amplitude, and phase distribution regulation, the state difference of power supply stability system of marine aquaculture DC brushless generator is calculated, and the fuzzy dispatch of power supply stability of marine aquaculture DC brushless generator is carried out by using nonlinear feedback regulation method:

$$\begin{cases} e_1(k) = x_1(k) - z_1(k) \\ e_2(k) = x_2(k) - z_2(k) \\ u_0(k) = k_p \mathrm{fal}\left(e_1(k), \alpha_1, \delta_1\right) + k_d \mathrm{fal}\left(e_2(k), \alpha_2, \delta_2\right) \\ u(k) = u_0(k) - \dfrac{z_3(k)}{b_0} \end{cases} \tag{6}$$

In the Eq. (6), α_1, α_2, δ_1, δ_2, and b_0 is the open-circuit voltage after the correction of DC brushless power generation in marine aquaculture; k_p, k_d is the proportion coefficient and differential coefficient of DC brushless power generation in marine aquaculture [8].

Using feedforward decoupling control, the oscillation characteristics in each control sampling period are assumed to be:

$$\begin{cases} \ddot{x}_1 = f_1\left(x_1, \dot{x}_1, x_2, \ddot{x}_2\right) + b_{11}u_1 + b_{12}u_2 \\ \ddot{x}_2 = f_2\left(x_1, \dot{x}_1, x_2, \ddot{x}_2\right) + b_{21}u_1 + b_{22}u_2 \\ y_1 = x_1, y_2 = x_2 \end{cases} \tag{7}$$

In the Eq. (7), y_i is the parameters of the marine aquaculture DC brushless generation pi regulator for the d_g channel, $f_i\left(x_1,\dot{x}_1,x_2,\ddot{x}_2\right),i=1,2$ is the dynamic coupling of marine aquaculture DC brushless generation, b_{ij} is the magnification factor of each frequency component of the DC brushless generation current in marine aquaculture [9], and the joint characteristic component of the DC brushless generation amplitude and phase angle in marine aquaculture is $b_{ij}\left(x,\dot{x},t\right)$. The system transfer matrix is:

$$B\left(x,\dot{x},t\right)=\begin{bmatrix} b_{11}\left(x,\dot{x},t\right) & b_{12}\left(x,\dot{x},t\right) \\ b_{21}\left(x,\dot{x},t\right) & b_{22}\left(x,\dot{x},t\right) \end{bmatrix} \tag{8}$$

where, $U=B\left(x,\dot{x},t\right)u$ represents the frequency of the harmonic component. The joint characteristic distribution of harmonic component and disturbance step between DC power generation in marine aquaculture is as follows:

$$\begin{cases} \ddot{x}_i=f_i\left(x_1,\dot{x}_1,x_2,\dot{x}_2,t\right)+U_i \\ y_i=x_i \end{cases} \tag{9}$$

The joint differential equations of the parameters of the DC power generation circuit and the parameters of the controller in marine aquaculture are as follows:

$$\begin{cases} \ddot{x}_1=f_1\left(x_1,\dot{x}_1,\cdots,x_m,\dot{x}_m\right)+U_1 \\ \ddot{x}_2=f_2\left(x_2,\dot{x}_2,\cdots,x_m,\dot{x}_m\right)+U_2 \\ y_1=x_1,y_2=x_2 \end{cases} \tag{10}$$

According to the above formula, the DC brushless adaptive coupling model of marine aquaculture DC brushless generator between different frequency systems is established for power supply stability.

3. Research on power supply stability

3.1. DC brushless adaptive coupling model

When the rectifier circuit of the generator system fails, the frequency component of the rectifier output voltage will change, with some frequency components suppressed and others enhanced. Therefore, compared with normal operation, the energy of the signal in the same frequency band is quite different, which means that the energy of each frequency band signal contains abundant fault information, and the change of some or several frequency band energy represents a fault situation. Based on this, this paper proposes a fault diagnosis method of rectifier circuit with "energy-failure" as the core idea. Fig. 5 shows the frame diagram of generator operating condition detection.

Based on the design of the parameters of the control constraint parameters model of the marine aquaculture DC brushless generator [10], the output load oscillation adjustment method is adopted to adjust the DC brushless self-adaptive steady state of the marine aquaculture DC brushless generator. The error control term is as follows:

$$L_x=\left(1-k_2\right)L_{11} \tag{11}$$

$$L_{\mathrm{mx}}=k^2L_{11} \tag{12}$$

$$n_x=k\sqrt{\frac{L_{11}}{L_{22}}} \tag{13}$$

Taking the amplitude of the interharmonic component as the constraint parameter and the controlled sampling

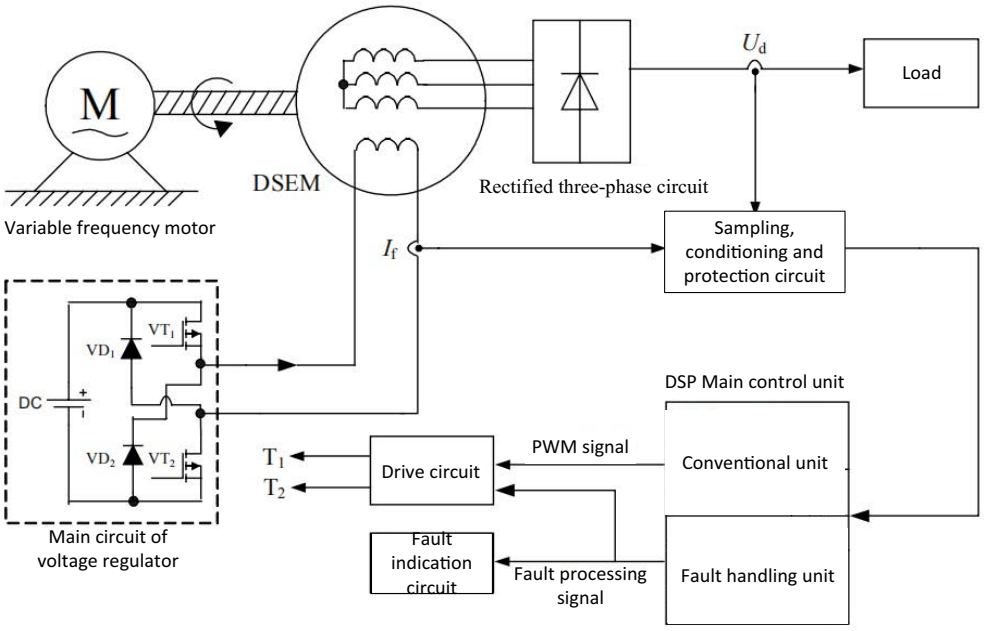

Fig. 5. Generator operating state diagnosis system.

period as the input, the impedance matching of the DC brushless generator for marine aquaculture is carried out during the controlled sampling period at the resonant point [11], and the characteristic of the power supply random analysis is as follows:

$$\omega_0 = \frac{1}{\sqrt{L_{lx}C_x}} = 2\pi f_0 \tag{14}$$

$$Z_0 = \sqrt{\frac{L_{lx}}{C_x}} = \omega_0 L_{lx} = \frac{1}{\omega_0 C_x} \tag{15}$$

The output power is used as the control objective function to optimize the power supply stability of marine aquaculture DC brushless generator to realize the power decoupling control [12].

Using the equal power Pike transform, the magnetic conductivity of the marine aquaculture DC brushless generator is as follows:

$$i_{\text{sec}}(t) = n_x\left[i_{\text{pri}}(t) - i_{L_{\text{mx}}}(t)\right] \tag{16}$$

The above equations are solved vertically, and the electric loss and magnetic loss of the marine aquaculture DC brushless generator are used as constraints to prepare the DC brushless adaptive distribution control design [13].

3.2. Marine aquaculture DC brushless generator power supply stability law

The DC brushless adaptive coupling model of marine aquaculture DC brushless generator with different frequency systems is established. The output constrained parameter model of DC brushless generator with DC brushless adaptive decoupling control is obtained by using multi-dimensional parameter adaptive fusion and steady-state tracking method:

$$I_{\text{pri}} = \frac{\pi}{4\omega L_{\text{mx}}}\frac{\cos(\alpha)}{\cos(x)\sin(x)}V_{\text{DC}} \tag{17}$$

$$I_o = \frac{2}{\pi}n_x\cos(x)I_{\text{pri}} \tag{18}$$

$$V_o = R_{\text{load}}I_o \tag{19}$$

wherein

$$x = \alpha - \theta = \tan^{-1}\left(\frac{n_x^2 R_{\text{load}}}{\omega L_{\text{mx}}}\right) \tag{20}$$

$$\alpha = \tan^{-1}\left(\left(\frac{\pi^2}{8n_x^2 R_{\text{load}}}\frac{\omega L_{\text{lmx}} - \frac{1}{\omega C_x}}{\cos^2(x)} + \tan(x)\right)\right) \tag{21}$$

$$\theta = \alpha - x \tag{22}$$

Error correction of output power distribution control under synchronous rotating coordinate system. The power supply stability model of marine aquaculture DC brushless generator satisfies $G_m(s) = G_0(s)$, $t_m = \tau$, the output voltage of inverter is calculated, and the optimal control law is:

$$H(s) + Y(s) = G_m(s)U(s) \tag{23}$$

Using Smith control system for multi-parameter fusion decoupling adjustment, the power supply stability of marine aquaculture DC brushless generator is affected by the interference vector $e^{-t_m s}$, and the tracking coupling control is taken as the optimized object. The characteristic equation of multi-power distribution control is as follows:

$$\frac{Y(s)}{R(s)} = \frac{G_C(s)G_0(s)e^{-\tau s}}{1 + G_C(s)G_0(s)} \tag{24}$$

Marine aquaculture DC brushless generator current ring control transfer function is:

$$Y(s) = \frac{e^{-L_m s}}{(\lambda_1 s + 1)}R(s) + \frac{(\lambda_2 s + L_m)s}{(\lambda_2 s + 1)}D(s) \tag{25}$$

Considering the effect of DC brushless generator modulation signal of marine aquaculture on DC side energy, the controller parameters have the following characteristic equations:

$$\frac{Y(s)}{R(s)} = \frac{G_C(s)G_0(s)e^{-\tau s}}{1 + G_C(s)G_m(s) + G_C(s)(G_0(s)e^{-\tau s} - G_m(s)e^{-t_m s})} \tag{26}$$

Under the condition of maximum power output gain, the output gain $K = \Delta K \cdot K_m$ of power supply stability of marine aquaculture $\Delta K > 0$ brushless generator is obtained. In the above analysis, the multi-dimensional parameter adaptive fusion and steady-state tracking method are used to adjust the DC brushless adaptive gain, and the inter-DC harmonic fluctuation of the marine aquaculture DC brushless generator is suppressed to achieve the power supply stability [14].

4. Analysis of simulation experiment

In order to test the application performance of this method in realizing the power supply stability of marine aquaculture DC brushless generator. Performance testing experiments are required, where the power supply environment is shown in Fig. 6.

The maximum power value of marine aquaculture DC brushless generator is 450 kW, the target power is 500 kW, the response time of the whole station power regulation is 24 ms, the resonant current of marine aquaculture DC brushless generator is 200 A, the phase inductance is 11 mH, the no-load start time of marine aquaculture brushless DC generator is 0.1 s, the duty ratio of the controllable variable of Boost-MMDCT is 0.25. At the same time, to facilitate the observation of data changes, the above data input to the PC end, where the data display interface is shown in Fig. 7.

Fig. 6. Marine aquaculture power supply environment.

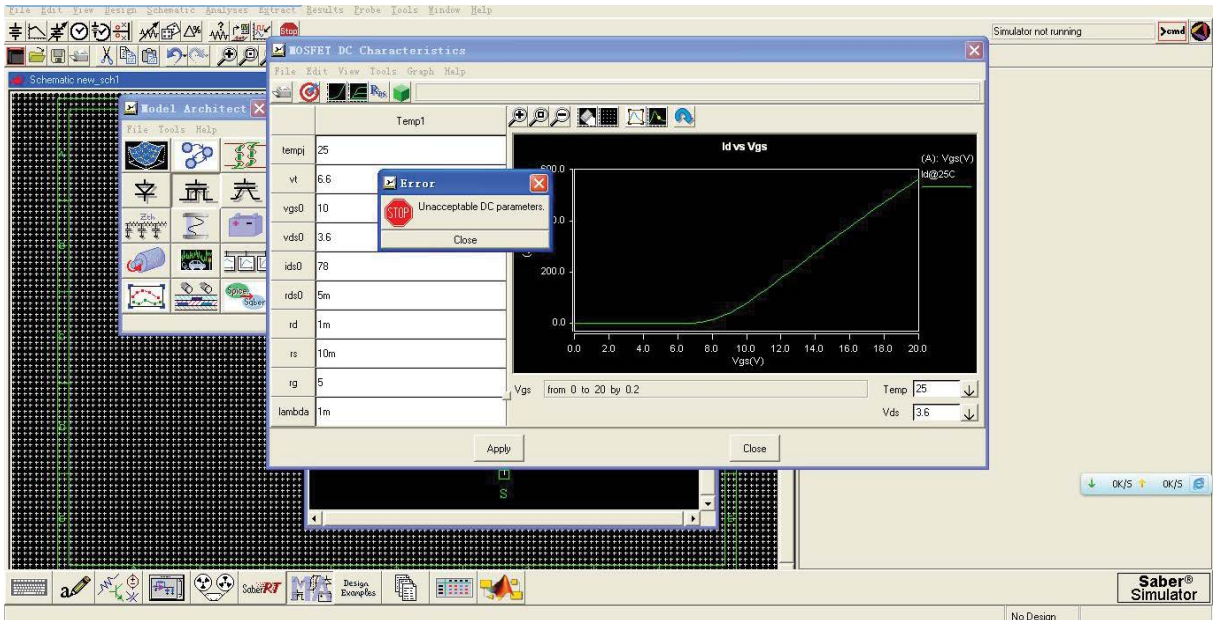

Fig. 7. Data display interface.

According to the above simulation parameter setting, the power supply stability of marine aquaculture brushless DC generator is tested with different series of the current system.

The analysis of Fig. 8 shows that the power supply stability can be effectively realized by this method, the output load is high, and the output power gain is tested. The result is shown in Fig. 9. The analysis of Fig. 9 shows that the output power gain of the power supply stability of the marine aquaculture DC brushless generator is higher and the performance is better.

At the rotational speed of 6,000 rpm, the output voltage ripple and ripple coefficient varying with the excitation current at no load is measured, as shown in Fig. 10. The voltage ripple situation at 270 V constant voltage output at different load currents is shown in Fig. 11. The measured results are basically consistent with the law of theoretical analysis, which verifies the correctness of the theoretical analysis.

Compared with the simulation results, the measured ripple value is larger than the simulation results, except for the two-dimensional finite element calculation error and

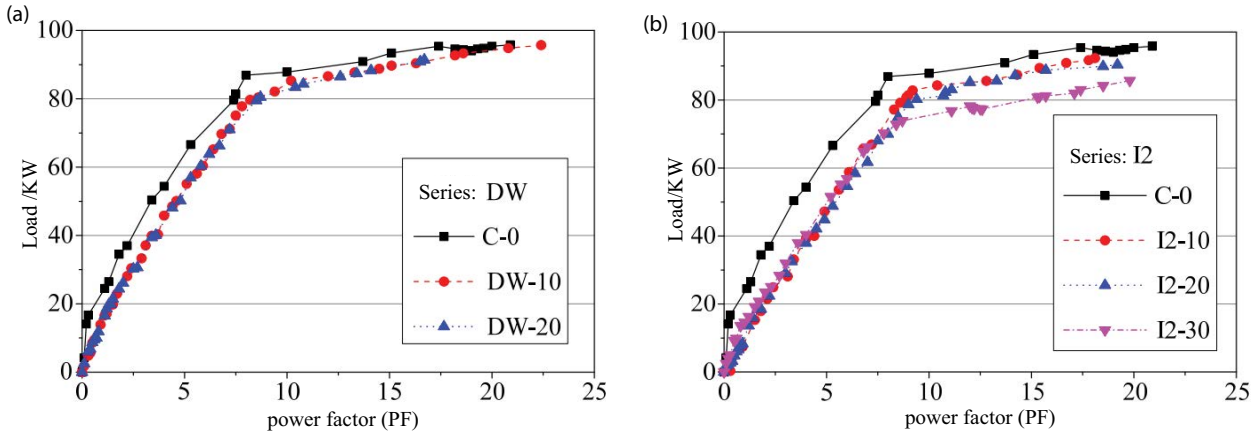

Fig. 8. DC brushless output load of marine aquaculture DC brushless generator: (a) DC and (b) AC marine aquaculture DC brushless generator series.

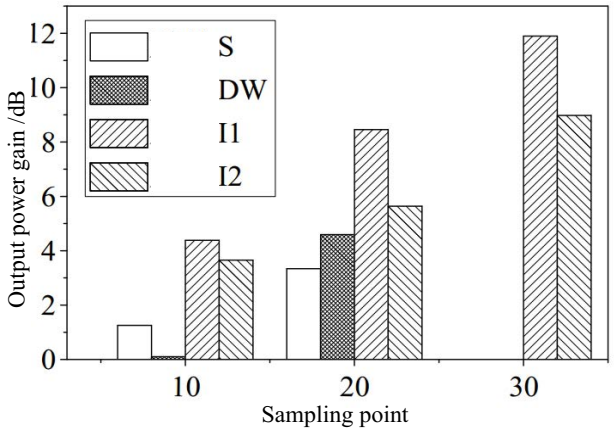

Fig. 9. Output power gain test.

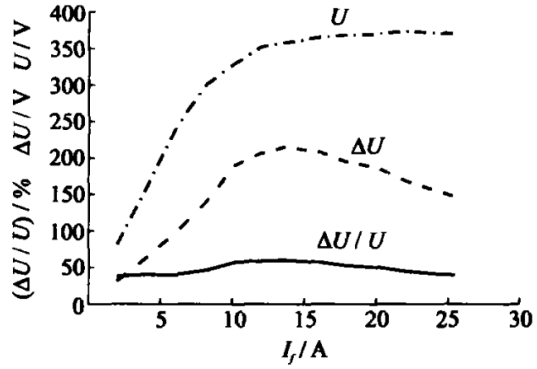

Fig. 10. Relationship between steady-state DC voltage and excitation current.

modeling error, the main reason is that the ripple effect of the excitation current caused by the fluctuation of the applied excitation power supply and the inductive potential of the excitation circuit and the effect of the rectifier converter are not considered in the simulation [15–17].

Based on the above contents, the power supply stability of marine aquaculture is analyzed. In this paper, the voltage signal will be detected at different locations of the power supply station, and the power supply stability will be judged based on this, and the detection results are shown in Fig. 12.

The voltage signal fluctuation of the rectifier circuit of the generator is less than 1 V. It can be judged that the generator is in stable operation at this time.

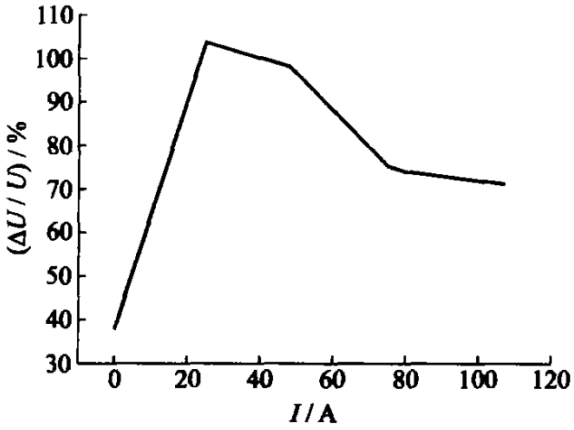

Fig. 11. Variation of load current at constant voltage.

5. Conclusions

For the multi-power decentralized control design of marine aquaculture DC brushless generator to improve the output power gain and stability of marine aquaculture DC brushless generator, this paper presents a power supply stability control method for marine aquaculture DC brushless generator based on multi-parameter fusion decoupling regulation. The nonlinear feedback adjustment method is used to fuzzy dispatch the power supply stability of marine aquaculture DC brushless generator, and to control the power supply stability by controlling the DC harmonic fluctuation of marine aquaculture DC brushless generator. The results

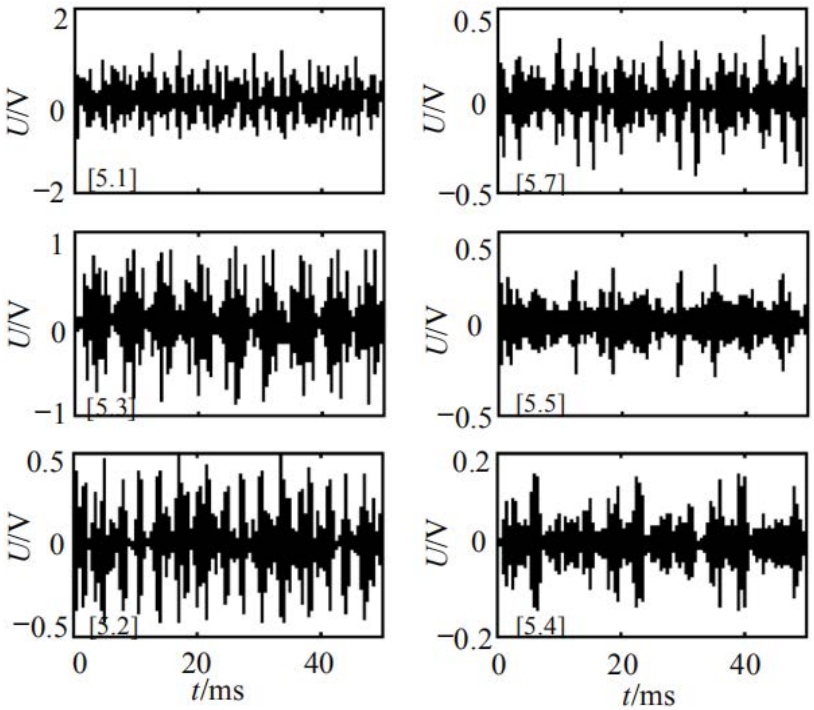

Fig. 12. Peak voltage signals at different sampling points.

show that the power supply stability, gain, and distribution control ability of DC brushless generator are high.

Acknowledgement

The research is supported by: Hunan Natural Science Foundation (No. 2018JJ356); Youth Project of Hunan Provincial Department of Education (No. 18B411).

References

[1] Y. Xu, K. Hong, J. Tsujii, E.I.-C. Chang, Feature engineering combined with machine learning and rule-based methods for structured information extraction from narrative clinical discharge summaries, J. Am. Med. Inf. Assoc., 19 (2012) 824–832.
[2] H.L. Roitblat, A. Kershaw, P. Oot, Document categorization in legal electronic discovery, computer classification vs. manual review, J. Assoc. Inf. Sci. Technol., 61 (2010) 70–80.
[3] Y. Yuan, F.Y. Wang, Blockchain, the state of the art and future trends, Acta Autom. Sin., 42 (2016) 481–494.
[4] P. He, G. Yu, Y.F. Zhang, Y.B. Bao, Survey on blockchain technology and its application prospects, Comput. Sci., 44 (2016) 1–7, 15.
[5] E. Turibamwe, R. Wangalwa, A comparative study of two biological monitoring systems in assessing water quality: a case of river Birira, Sheema District, Uganda, Water Conserv. Manage., 4 (2020) 07–14.
[6] A. Maqbool, W. Hui, M.T. Sarwar, Nanotechnology development for *in-situ* remediation of heavy metal (Loid)S contaminated soil, Environ. Ecosyst. Sci., 3 (2019) 09–11.
[7] Z.B. Siew, C.M.M. Chin, N. Sakundarini, Designing a guideline for green roof system in Malaysia, J. Clean WAS, 3 (2019) 05–10.
[8] X.K. Sun, Z.Y. Peng, X.L. Guo, Some characterizations of robust optimal solutions for uncertain convex optimization problems, Optim. Lett., 10 (2016) 1463–1478.
[9] W.X. Yao, Research on the policy effect of incremental expansion of margin and securities lending, based on the multi period DID model and Hausman's test, Int. Financ. Res., 349 (2016) 85–96.
[10] Y.Y. Jin, S.B. Jia, Study on the influence of the introduction of leverage ratio on the asset structure of commercial banks, Int. Financ. Res., 350 (2016) 52–60.
[11] A.C. Jia, G. Zhou, Study on selection of suppliers based on rough set and BP neural network, Logist. Technol., 31 (2012) 229–232.
[12] Q.Y. Zhang, R.C. Wang, C. Sha, H.-p. Huang, Node correlation clustering algorithm for wireless multimedia sensor networks based on overlapped FoVs, J. China Univ. Posts Telecommun., 20 (2013) 37–44.
[13] M. Zhu, S. Liu, J. Jiang, A hybrid method for learning multi-dimensional Bayesian network classifiers based on an optimization model, Appl. Intell., 44 (2016) 1–26.
[14] Z. Liu, Y. Yuan, X. Guan, X. Li, An approach of distributed joint optimization for cluster-based wireless sensor networks, IEEE/CAA J. Autom. Sin., 2 (2015) 267–273.
[15] J.M. Yang, Y.H. Hou, H. Sun, Z.W. Zhao, Modified NSGA-II-DE with two-dimensional information ordering strategy and magnitude threshold, Control Decis., 31 (2016) 1577–1584.
[16] S.S. Sun, S. Wang, Z.F. Fan, Flow scheduling cost based congestion control routing algorithm for data center network on software defined network architecture, J. Comput. Appl., 36 (2016) 1784–1788.
[17] Q.Y. Zhu, X.F. Yang, L.-X. Yang, C. Zhang, Optimal control of computer virus under a delayed model, Appl. Math. Comput., 218 (2012) 11613–11619.